Global Change Biology (2005) **11,** 619–632, doi: 10.1111/j.1365-2486.2005.00930.x

A generalized, bioclimatic index to predict foliar phenology in response to climate

WILLIAM M. JOLLY*, RAMAKRISHNA NEMANI† and STEVEN W. RUNNING*
*NTSG, College of Forestry and Conservation, SC428, University of Montana, Missoula, MT 59812, USA,
†NASA AMES Research Center, Moffett Field, CA 94035, USA

Abstract

The phenological state of vegetation significantly affects exchanges of heat, mass, and momentum between the Earth's surface and the atmosphere. Although current patterns can be estimated from satellites, we lack the ability to predict future trends in response to climate change. We searched the literature for a common set of variables that might be combined into an index to quantify the greenness of vegetation throughout the year. We selected as variables: daylength (photoperiod), evaporative demand (vapor pressure deficit), and suboptimal (minimum) temperatures. For each variable we set threshold limits, within which the relative phenological performance of the vegetation was assumed to vary from inactive (0) to unconstrained (1). A combined Growing Season Index (GSI) was derived as the product of the three indices. Ten-day mean GSI values for nine widely dispersed ecosystems showed good agreement ($r > 0.8$) with the satellite-derived Normalized Difference Vegetation Index (NDVI). We also tested the model at a temperate deciduous forest by comparing model estimates with average field observations of leaf flush and leaf coloration. The mean absolute error of predictions at this site was 3 days for average leaf flush dates and 2 days for leaf coloration dates. Finally, we used this model to produce a global map that distinguishes major differences in regional phenological controls. The model appears sufficiently robust to reconstruct historical variation as well as to forecast future phenological responses to changing climatic conditions.

Keywords: climate change, global, minimum temperature, model, phenology, photoperiod, vapor pressure deficit

Received 23 June 2004 and accepted 4 November 2004

Introduction

For centuries, people have observed annual variation in the dates at which buds break and flowers bloom (Sparks & Carey, 1995). The science of plant phenology is concerned with understanding the variability of these reproductive and vegetative cycles, particularly in relation to their biotic and abiotic forcings (Lieth, 1974). Plant vegetative cycles, such as the timing and duration of foliage, determine exchange periods of carbon dioxide and water between the Earth's surface and the atmosphere. Recent decades have seen changes in the timing and duration of plant greenness across much of the globe (Myneni *et al*., 1997; Menzel & Fabian, 1999; Schwartz & Reiter, 2000; Matsumoto *et al*., 2003) and these changes could have a large impact on the global carbon cycle (Keeling *et al*., 1996).

Correspondence: William M. Jolly, tel. +1 (406) 243 6230, fax +1 (406) 243 4510, e-mail: mattj@ntsg.umt.edu

Satellite observations, ground observations, and mathematical models are all key components that aid in the study of large-scale phenological patterns (Schwartz, 1999). Researchers have used satellite data to adequately map the waxing and waning of vegetation greenness across the Earth's surface (Justice *et al*., 1985). These phenological estimates have improved regional and interannual predictions from general circulation models (Chase *et al*., 1996), but such coupled land–atmosphere models often use fixed vegetation phenology parameters (Sellers *et al*., 1996). This neglects the dynamic characteristics of surface vegetation. Ground observations aid in developing a more dynamic link between driving variables, such as climate, and phenophase transitions, but these observations are generally not well distributed globally and the quality of such data is dependent on the skills of the observer (Menzel, 2002). Mathematical models bridge

the gap between the extensive spatial scales available from satellite-derived observations and the linkage to driving variables that can potentially be derived from ground observations. Work has been carried out to combine such phenology models as part of land-surface models that are then coupled with global climate models to provide dynamic, large-scale predictions of interactions between vegetation and climate, but this work would benefit from a more generalized and complete description of vegetation phenology (Foley *et al*., 1998).

Phenology models predict canopy greenness from climate data because climate is the primary driver at large scales (Botta *et al*., 2000). In the mid- and high latitudes, phenology is controlled by temperature and photoperiod (Myneni *et al*., 1997; White *et al*., 1997; Chuine & Cour, 1999; Jarvis & Linder, 2000; Schwartz & Reiter, 2000), but regionally, water limitations may also be important (Peñuelas *et al*., 2004). In the tropics, phenology is controlled either by seasonal rainfall (Childes, 1989; de Bie *et al*., 1998; Bach, 2002) or photoperiod (Njoku, 1958; Borchert & Rivera, 2001). However, single climatic factors do not always limit phenology at a given location; sometimes multiple factors control phenology concurrently or at different times of the year (Nilsen & Muller, 1981; White *et al*., 1997; Jame *et al*., 1998).

Foliar phenology models have been developed to predict dates of leaf flushing and leaf senescence from available climate data (Kramer, 1994; White, 1997 #19; Botta *et al*., 2000; Kang *et al*., 2003; Jolly & Running, 2004), but many of these models were developed for temperate ecosystems where phenophase transitions are easily defined. In the tropics, seasonal water availability promotes rapid leaf flushing while leaf senescence may occur gradually over as much as 6 months (Childes, 1989); any choice of a single-leaf senescence date would be arbitrary at best.

Attempts to model phenology globally have been constrained to the prediction of the start of leaf flushing, or onset, and have neglected the dynamics of leaf fall at the end of the growing season (Botta *et al*., 2000). In addition, continental or larger scale phenology models require *a priori* knowledge of the climate or vegetation in order to discretely switch among biome-specific models (White *et al*., 1997; Botta *et al*., 2000). This limits their utility for forecasting the impacts of climate change on vegetation because the limiting factor at a given location may change. An alternative to traditional phenology models might be to continuously characterize within-year variation in canopy leaf area, rather than finite phenophase transitions, by combining the limitations and interactions of *all* key climate variables into a single index of foliar phenology. This is possible if we assume that there are a minimum set of requirements that must be met for a plant to either initiate or maintain a certain phenological state.

In this paper, we seek to develop a simple, generalized phenology model to test the hypothesis that there is such a set of common climatic conditions that interact to limit foliar phenology globally. We are interested in predicting not only the beginning and end of the growing season but also the status of the canopy throughout the year without *a priori* knowledge of the vegetation or climate. We show that the model can also predict phenophase transition dates like traditional foliar phenology models. We seek to drive the model with readily available climatic data, and to provide an integrative index that combines the weighed effects of daylength (photoperiod), evaporative demand (vapor pressure deficit (VPD)), and suboptimal (minimum) temperature. We test the generality of the model at widely diverse locations and judge its performance against satellite-derived estimates of the Normalized Difference Vegetation Index (NDVI). We also test the model at a temperate deciduous forest site to assess its ability to predict interannual differences in leaf flush and leaf senescence dates.

Methods

Model development

We searched for a common set of meteorological variables that together might account for much of the variation observed in the seasonal phenology recorded across the Earth. We chose three that are readily available and good surrogates for the underlying mechanisms: low temperatures, evaporative demand, and photoperiod. From the literature, we extracted threshold limits for each variable, between assuming that phenological activity varied linearly from inactive (0) to unconstrained (1). These functions and their derivations are described in detail below. The product of the three indices forms a combined model that is calculated daily and integrated as a 21-day running average to avoid reaction to short-term changes in environmental conditions (Lieberman, 1982; Lechowicz, 2001).

Minimum temperature. Many of the biochemical processes of plants are sensitive to low temperatures (Levitt, 1980). Although ambient air temperatures certainly influence growth, constraints on phenology appear to be more closely related to restrictions on water uptake by roots when soil temperatures are

suboptimal (Waring, 1969). Many field studies show variable ecosystem responses over a range of minimum temperatures. Jarvis & Linder (2000) demonstrated that northern spruces and pines increase their photosynthesis rapidly once temperatures exceed −1 °C. Temperatures below freezing are lethal, however, for tropical trees (Larcher, 1995). Temperatures below −2 °C can freeze water in the xylem of some trees (Zimmerman, 1964). Minimum temperature is also a stronger indicator of climate change than either average or maximum temperature (IPCC, 2001). To incorporate a range of species, we chose a range encompassed by a lower minimum temperature threshold of −2 °C (T_{MMin}) and an upper threshold of 5 °C (T_{MMax}). A similar range of low-temperature sensitivities has been reported elsewhere (Larcher & Bauer, 1981).

A minimum temperature index (iT_{Min}), presented graphically in Fig. 1a, was created as follows:

$$iT_{Min} = \begin{cases} 0, & \text{if } T_{Min} \le T_{MMin}, \\ \dfrac{T_{Min} - T_{MMin}}{T_{MMax} - T_{MMin}}, & \text{if } T_{MMax} > T_{Min} > T_{MMin}, \\ 1, & \text{if } T_{Min} \ge T_{MMax}, \end{cases} \quad (1)$$

where iT_{Min} is the daily indicator for minimum temperature and is bounded between 0 and 1 and T_{Min} is the observed daily minimum temperature in degrees Celsius. For all tests, $T_{MMin} = -2$ °C and $T_{MMax} = 5$ °C.

VPD. Water stress causes partial to complete stomatal closure (Mott & Parkhurst, 1991), reduces leaf development rate (Salah & Tardieu, 1996), induces the shedding of leaves (Childes, 1989), and slows or halts cell division (Granier & Tardieu, 1999). Although models are available to calculate a soil water balance, they require knowledge of rooting depth, soil texture, latent heat losses, and precipitation. As a surrogate, we selected an index of the evaporative demand, the VPD of the atmosphere. At low values, latent heat losses are unlikely to exceed available water, whereas at high values, particularly if sustained, photosynthesis and growth are likely to be significantly limited. The distribution of vegetation with different phenological patterns is thus, very sensitive to seasonal changes in VPD (Huffaker, 1942).

From the literature, we find evidence that VPD less than 900 Pa should exert little effect on stomata whereas values greater than 4100 Pa generally are sufficient to force complete stomatal closure, even when the soils are moist (Osonubi & Davies, 1980; Tenhunen *et al.*, 1982). Although these limits vary by locations and species (White *et al.*, 2000), we chose a common set of parameters for all sites. The VPD index (*iVPD*), shown graphically in Fig. 1b, was, therefore, derived as follows:

$$iVPD = \begin{cases} 0, & \text{if } VPD \ge VPD_{Max}, \\ 1 - \dfrac{VPD - VPD_{Min}}{VPD_{Max} - VPD_{Min}}, & \text{if } VPD_{Max} > VPD > VPD_{Min}, \\ 1, & \text{if } VPD \le VPD_{Min}, \end{cases} \quad (2)$$

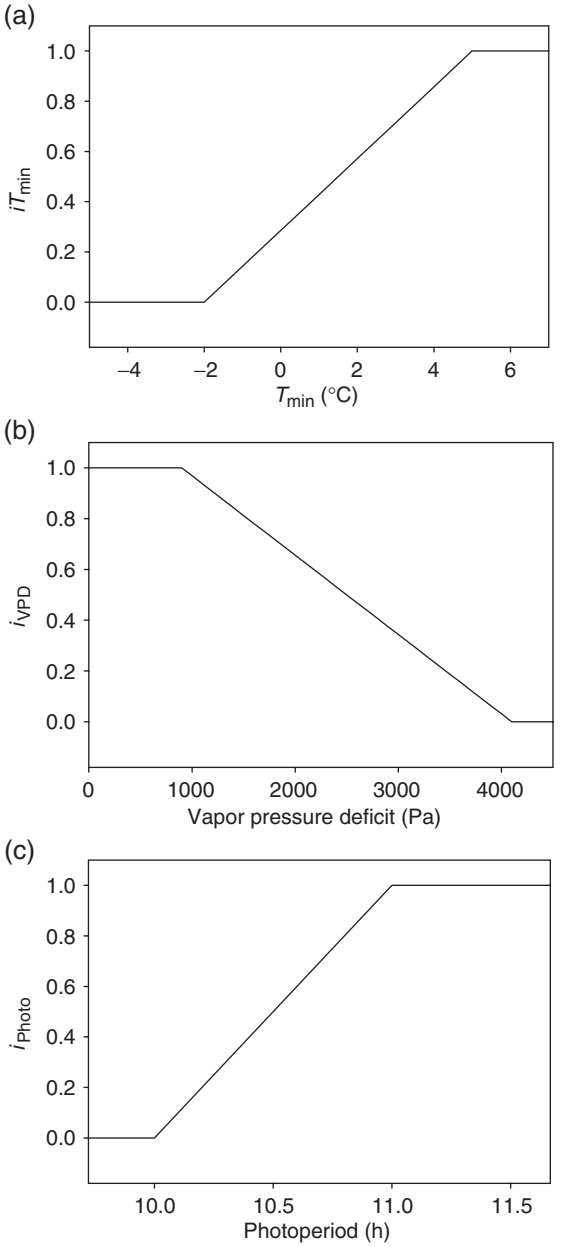

Fig. 1 Graphic representation of minimum temperature, vapor pressure deficit, and photoperiod indicator functions used to predict foliar phenology. For each variable, threshold limits are defined, between which the relative constraint on phenology is assumed to vary linearly from inactive (0) to unconstrained (1).

where *iVPD* is the daily indicator for VPD and is bounded between 0 and 1 and *VPD* is the observed daily VPD in Pascals. For all tests, $VPD_{Min} = 900$ Pa and $VPD_{Max} = 4100$ Pa.

Photoperiod. Photoperiod provides a plant with a reliable annual climatic cue because it does not vary from year to year at a given location. We assume that photoperiod provides the outer envelope within which other climatic controls may dictate foliar development. Studies have shown that photoperiod is important to both leaf flush and leaf senescence throughout the world (Njoku, 1958; Rosenthal & Camm, 1997; White *et al*., 1997; Hakkinen *et al*., 1998; Partanen *et al*., 1998; Borchert & Rivera, 2001). Photoperiod also interacts with temperature to limit foliar phenology, rendering temperature changes ineffective without corresponding photoperiod changes (Partanen *et al*., 1998). We assumed photoperiods of 10 h or less completely limited canopy development and 11 h or more allowed canopies to develop unconstrained. The photoperiod index (*iPhoto*), shown graphically in Fig. 1c, was, therefore, derived as follows:

$$iPhoto = \begin{cases} 0, & \text{if } Photo \le Photo_{Min}, \\ \dfrac{Photo - Photo_{Min}}{Photo_{Max} - Photo_{Min}}, & \text{if } Photo_{Max} > Photo > Photo_{Min}, \\ 1, & \text{if } Photo \ge Photo_{Max}, \end{cases} \quad (3)$$

where *iPhoto* is the daily photoperiod indicator and *Photo* is the daily photoperiod in seconds. For all tests, $Photo_{Min} = 36\,000$ s (10 h) and $Photo_{Max} = 39\,600$ s (11 h).

The Growing Season Index (GSI)

The product of the individual daily indicators for minimum temperature, VPD, and photoperiod forms a single metric which can be monitored for canopy greenness, hereafter referred to as the GSI. The GSI is a daily indicator of the relative constraints to foliar canopy development or maintenance due to climatic limits. It is continuous but bounded between 0 (inactive) and 1 (unconstrained). The daily metric (*iGSI*) is calculated as follows:

$$iGSI = iT_{min} \times iVPD \times iPhoto, \quad (4)$$

where *iGSI* is the daily GSI, iT_{min} is the minimum temperature indicator, *iVPD* is the VPD indicator, and *iPhoto* is the photoperiod indicator. The daily GSI is then calculated as the 21-day moving average of daily indicator, *iGSI*, for all sites. The moving average serves to buffer single extreme events from prematurely triggering canopy changes.

Table 1 Location and description of model test sites and their respective vegetation types from the WWF Ecoregions map

WMO ID	Site name	Location	Biome	Lat. (DD)	Lon. (DD)	Elev. (m)
228870	Russia	Scandinavian and Russian taiga	Boreal forests/Taiga	61.2	46.7	56
443020	Mongolia	Mongolian–Manchurian grassland	Temperate grasslands, savannas, and shrublands	47.8	112.1	926
610360	Sahel	Sahelian Acacia savanna	Tropical and subtropical grasslands, savannas, and shrublands	14.2	1.5	210
682260	Kalahari	Kalahari xeric savanna	Deserts and Xeric shrublands	−24.0	21.9	1100
701718	Alaska	Interior Alaska/Yukon lowland taiga	Boreal forests/Taiga	67.1	−157.9	88
727730	Missoula	North-Central Rockies forest	Temperate Conifer forest	46.9	−114.1	972
726165	Harvard Forest	New England/Acadian forests	Temperate broadleaf and mixed forests	42.9	−72.3	149
833620	Cerrado	Cerrado	Tropical and subtropical grasslands, savannas and shrublands	−15.6	−56.1	182
943320	Australia	Mitchell grass downs	Tropical and subtropical grasslands, savannas, and shrublands	−20.7	139.5	344

Lat., latitude; Lon., longitude; Elev., elevation.

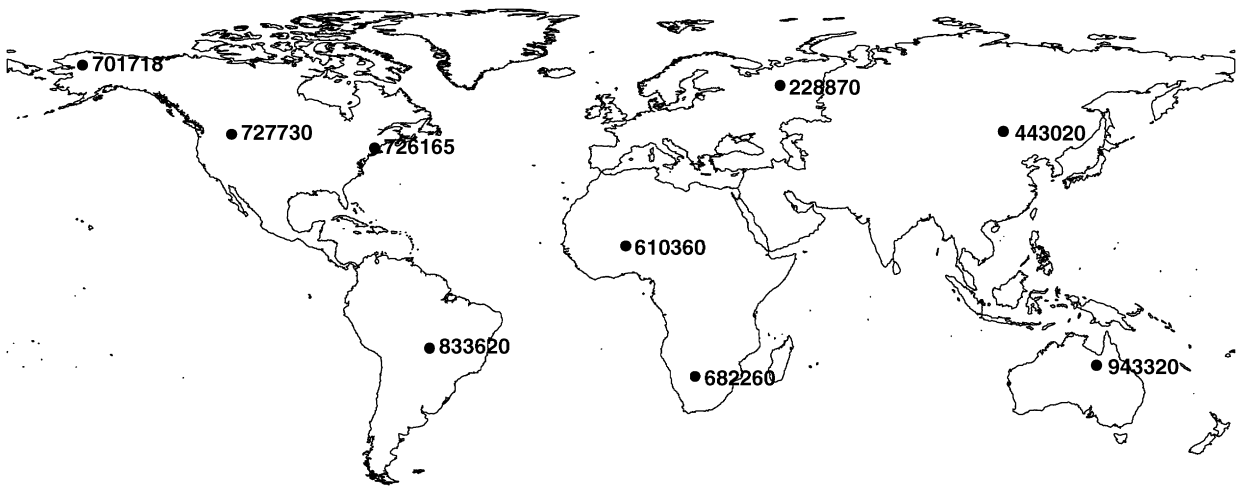

Fig. 2 Location of test sites, designated by the weather station identification provided by the World Meteorological Office.

Model test sites. Nine global sites were selected to represent a range of phenologically different biomes. At least one site was selected per continent, excluding Antarctica, with additional sites selected to provide a range of biome types. Site vegetation was determined from the World Wildlife Foundation (WWF) map of global ecoregions (Olson *et al.*, 2001). A summary of these site locations and their related biome types is shown in Table 1 and their spatial distribution is shown in Fig. 2.

Meteorological data. Meteorological data were extracted from the National Climate Data Center Global Summary of the Day from January to December for 2000 if sites were in the northern hemisphere, and from July to June for 1999–2000 if sites were in the southern hemisphere, except at the Australia site where intra-annual variability was best expressed over the calendar year 2000 because of peak vegetation activity in May. Only average temperature, minimum temperature, and dewpoint temperature were required. Daily VPDs were estimated for each site as the difference between saturation vapor pressure and actual vapor pressure estimated using average temperature and dewpoint temperature, respectively, with a standard relationship between temperature and vapor pressure (Campbell & Norman, 1998). The daily photoperiod was estimated using site latitude and yearday (Monteith & Unsworth, 1990).

Satellite Data. NDVIs were extracted from the NOAA/NASA Pathfinder AVHRR Land (PAL) global, 10-day, 8 km resolution composite dataset. PAL NDVI values were resampled to 0.25° using a spatial average to reduce the impacts of atmospheric contamination. NDVI has been shown to be strongly related to leaf area index (LAI) (Myneni *et al.*, 1995) and should provide a suitable means by which to test model intra-annual canopy dynamics. We selected the raster value closest to each site, based on latitude and longitude, and extracted an NDVI corresponding to the meterological dataset. The NDVI time series were filtered using a five composite period moving average of NDVI to remove spurious increases and decreases in NDVI caused by atmospheric contamination (Lovell & Graetz, 2001).

Model comparisons with NDVI. GSI values were calculated daily at each site using the model parameters and logic shown in Eqns (1)–(4). For comparison with satellite data at each site, we calculated the mean GSI for the corresponding 10-day satellite data composite period and compared these means with satellite-derived NDVI with a standard Pearson's product–moment correlation.

Model comparisons with phenology observations at Harvard Forest. We also estimated GSI values for Harvard Forest using weather data derived from the DAYMET meteorological archive (Thornton *et al.*, 1997, http://www.daymet.org) and compared these simulations with phenological field observations. The same model parameters and logic shown in Eqns (1)–(4) were used for this analysis. Phenology observations were averaged over all species for each observation date. The average date of leaf flushing, or onset, was defined as the time when average canopy leaf area exceeded 10% of the seasonal maximum. Conversely, the average date of leaf coloration, or offset, was defined as the date when leaf coloration exceeded 90%. Model simulations

were performed daily from 1990 to 1997. Modeled leaf onset was defined as the time when GSI exceeded 0.5 in the spring and leaf offset was defined as the time when GSI dropped below 0.5 in the fall. We computed the mean absolute error (MAE) as the difference between the predicted and observed yeardays of leaf onset and leaf offset. Model predicted leaf onset dates were compared with average observed leaf onset dates for 1990–1997. Model-predicted leaf offset dates were compared with average observed leaf offset dates for 1991–1997. Our analysis was limited to this range of dates because of differences in data availability for both DAYMET and phenology observations.

Mapping global controls on vegetation foliar phenology

We used our generalized phenology model to calculate the relative annual controls of VPD, minimum temperature, and photoperiod spatially over the entire globe. We utilized daily gridded climate data from the National Center for Environment Prediction (NCEP)/National Center for Atmospheric Research (NCAR) Reanalysis (Kistler *et al*., 2001) for the year 2000 to construct a global map of the factors that limit foliar phenology. We calculated the point-wise daily indicators for minimum temperature, VPD, and photoperiod (Eqns (1)–(3), respectively) and summed each indicator over the year. These indicators tell us the number of days of the year that each variable was not limiting at a given location. We then subtracted the annual point-wise indicator sums from 365 to express each value in terms of the number of days that it limits phenology in a year. We calculated the actual vapor pressure from surface air pressure and specific humidity and saturation vapor pressure from average surface temperature. VPD was calculated as the difference between saturation and actual vapor pressures. Photoperiod was estimated as a function of latitude and yearday (Monteith & Unsworth, 1990). The temperature, VPD, and photoperiod limits were then displayed as an Red/Green/Blue (RGB) composite with each color representing a variable. VPD limits are displayed in red, photoperiod limits are displayed in green and minimum temperature limits are displayed in blue.

Table 2 Correlations between composite period NDVI values and modeled GSI values averaged over the composite period for each of the nine test sites

WMO ID	Location	Correlation between GSI and NDVI
228870	Russia	0.939
443020	Mongolia	0.903
610360	Sahel	0.896
682260	Kalahari	0.742
701718	Alaska	0.986
726165	Harvard Forest	0.870
727730	Missoula	0.839
833620	Cerrado	0.868
943320	Australia	0.571

All correlations were significant ($P < 0.001$).
NDVI, Normalized Difference Vegetation Index; GSI, Growing Season Index; WMO, World Meteorological Office.

Results

The correlations between model-predicted GSI values and satellite-derived NDVI values are shown in Table 2. Using the same model and the same parameters we were able to adequately predict the intra-annual dynamics of the vegetation canopy at all sites regardless of the dominant or co-dominant climatic controls at that site. There was a slight, but not marked, bias towards better predictions at temperate sites. The highest correlations were found in the high-latitude forests, presumably because they are more purely temperature limited than other sites. However, correlations at the hydroperiodic sites were still very high, suggesting that the VPD control adequately depicts the intra-annual canopy dynamics in these regions.

Individual daily index values for minimum temperature, VPD, and daylength at each site are shown in Fig. 3. These figures clearly show the relative influence of water, light, and temperature limitations at each site. In only two cases does a single variable limit foliar phenology (Fig. 3c, h). More often, there is a mix of environmental limits both temporally, as shown when observed over time at a given site, and spatially, as shown when comparing sites.

Time-series plots of model-predicted foliar phenology and NDVI values for each site are shown in Fig. 4. In all cases, regardless of the previously reported correlations, the GSI-predicted canopy dynamics appear to correspond well with observed canopy changes. In some cases, the model predicted a drop in canopy greenness after the initial start-of-season increase. For example, at the Mongolia site, the start-of-season is determined from temperature limits but the growing season has high VPD. This is shown clearly in Fig. 3b where the large red areas in midsummer indicate water stress. During the period of the predicted canopy activity drop, the rate of increase of NDVI is less than the early season, suggesting that this VPD control may be important in determining the rate of canopy increase. In the Kalahari, early season conditions that were not limiting were not met with concurrent increases in canopy greenness. However, small concomitant increases and decreases between NDVI and

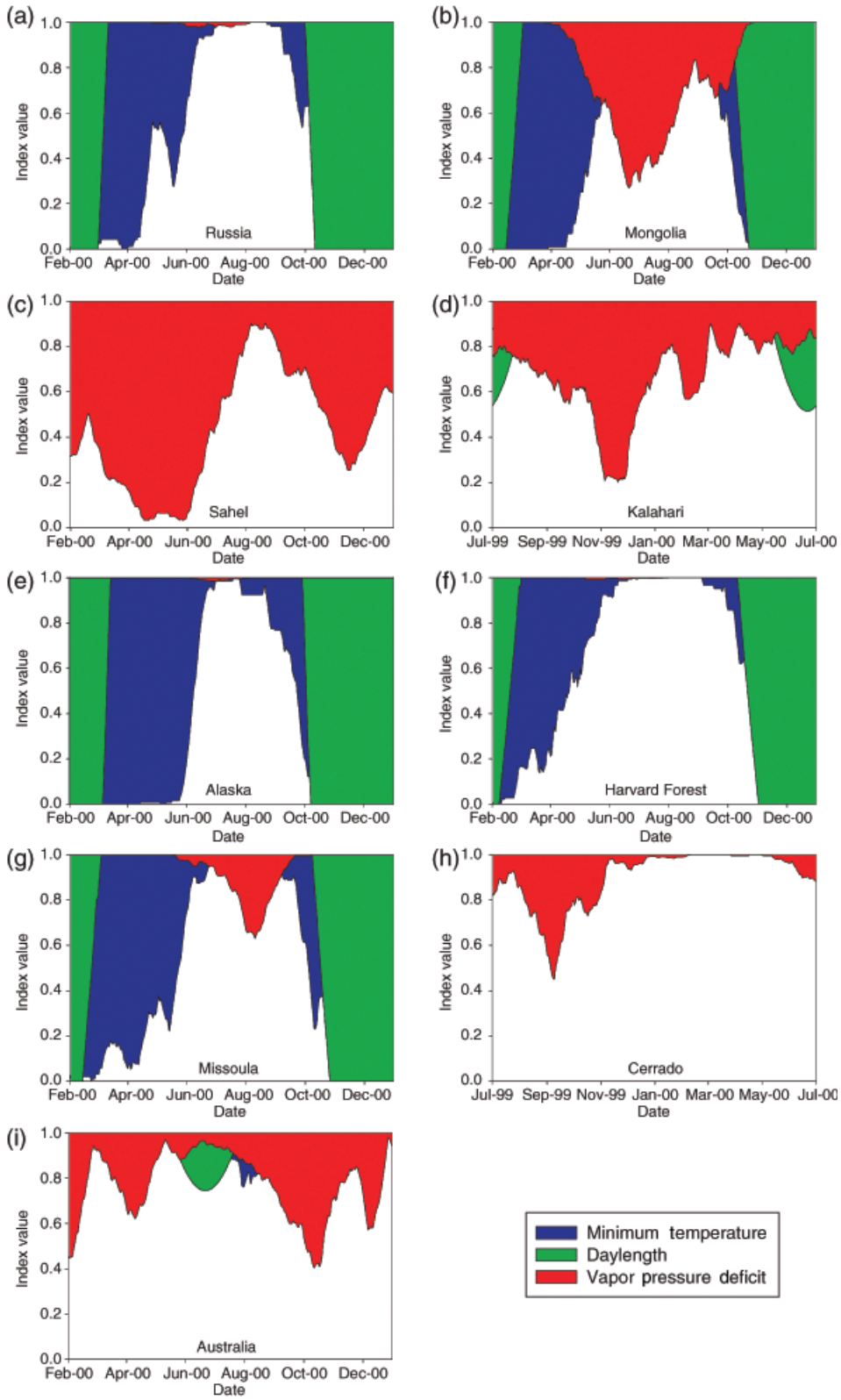

Fig. 3 The seasonal index values for minimum temperature, vapor pressure deficit, and daylength for each site showing the seasonal limits of each variable. Indices are presented as a 21-day running average to better depict seasonal trends.

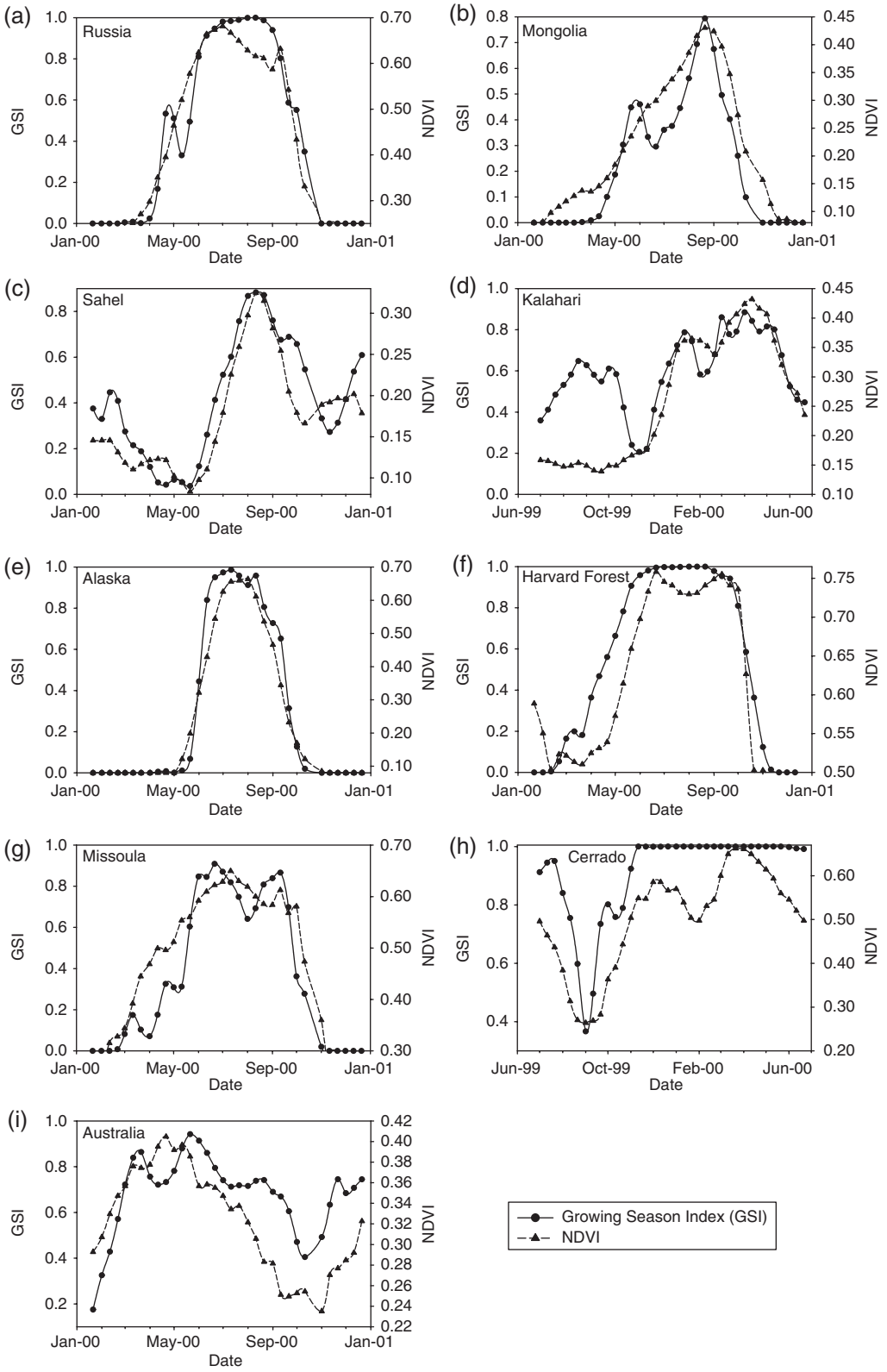

Fig. 4 A comparison of seasonal variation in the modeled Growing Season Index (GSI) with the Normalized Difference Vegetation Index (NDVI) obtained from satellite coverage at 10-day intervals (see correlation coefficients in Table 2).

Table 3 Differences between model predicted and field observed average leaf onset dates for Harvard Forests from 1990 to 1997

Observed average onset date	Predicted onset date	Absolute difference
4/28/1990	5/1/1990	3
4/16/1991	4/24/1991	8
5/1/1992	5/6/1992	5
4/24/1993	4/25/1993	1
4/28/1994	4/30/1994	2
5/3/1995	5/3/1995	0
4/25/1996	5/2/1996	7
5/5/1997	5/6/1997	1
	MAE (days)	3.38

The mean absolute error (MAE) of the model predictions was 3.38 days.

Table 4 Differences between model predicted and field observed average leaf offset dates for Harvard Forests from 1991 to 1997

Observed average offset date	Predicted offset date	Absolute difference
10/23/1991	10/25/1991	2
10/23/1992	10/20/1992	3
10/18/1993	10/19/1993	1
10/21/1994	10/20/1994	1
10/24/1995	10/28/1995	4
10/21/1996	10/22/1996	1
10/28/1997	10/24/1997	4
	MAE (days)	2.29

The mean absolute error (MAE) of the model predictions was 2.29 days.

GSI values are observed during that period and the model predicts a clear leaf flush as conditions become more favorable. At Harvard Forest, the model over-predicts increases in timing of observed increases in canopy leaf area. However, modeled changes in canopy greenness generally track well with observed changes in canopy leaf area at all sites.

The results of model estimates of leaf onset compared with observations is shown in Table 3 and leaf offset comparisons are shown in Table 4. There was good agreement between the modeled leaf onset and offset dates and observations at Harvard Forest. The MAE of predicted onset date compared with observed mean onset date over 8 years was 3.38 days and the MAE of predicted offset date over 7 years was 2.29 days. These accuracies should not be overstated because a simple mean yields an MAE of 4.25 and 2.14 days for onset and offset, respectively. However, observed onset dates were twice as variable as observed offset dates (standard deviation of 6 days for onset compared with 3 days for offset), while prediction errors only differed by about 1 day, suggesting that the model is robust to interannual variability. This suggests that even though the model predicts continuous changes in canopy activity, it still serves well as a model to predict the start and end dates of the foliage period.

The map of global climatic constraints to foliar phenology is shown in Fig. 5. This map resolves major global patterns of phenology while also revealing some interesting patterns of interactive effects. Black areas in the tropics show regions where climate is essentially aseasonal; red areas show where water limits dominate foliar phenology; blue shows where minimum temperatures most limit phenology. Blue-green and green-blue areas have co-limitations of photoperiod and temperatures. The patterns depicted are consistent with the global distribution of biomes that exhibit vastly different leaf phenological strategies.

Discussion

In this paper, we have presented a new way of assessing canopy foliar dynamics by combining simple environmental limitations into an index that quantifies changes in those limitations within the year. We have succeeded in reproducing the intra-annual canopy dynamics seen from satellite-derived vegetation indices in various regions throughout the world, independent of vegetation type, while using the same type of input data, the same model and the same model parameters. The model performs well in multiple locations because it does not impose *a priori* knowledge of vegetation or climate to switch discretely between models or model parameters; it simply allows controlling climatic factors to shift or co-limit both temporally and spatially.

A key component to this model, which promotes its application to climate change scenarios, is this ability to transition from one limiting factor to another without the need for a discrete model change. As mentioned earlier, previous attempts to model vegetation phenology globally have required the discrete switching from one model to another (Botta *et al*., 2000). Even in regions that are small compared with the entire globe, different factors limit foliar phenology spatially (Peñuelas *et al*., 2004). Therefore, a generalized phenology model must provide sufficient flexibility to transition from one limiting factor to another in both space and time.

In some cases, the model seemed to predict suitable conditions when no observed changes in canopy were evident. In the Kalahari, early season VPDs were low and photoperiods were long, but no canopy changes

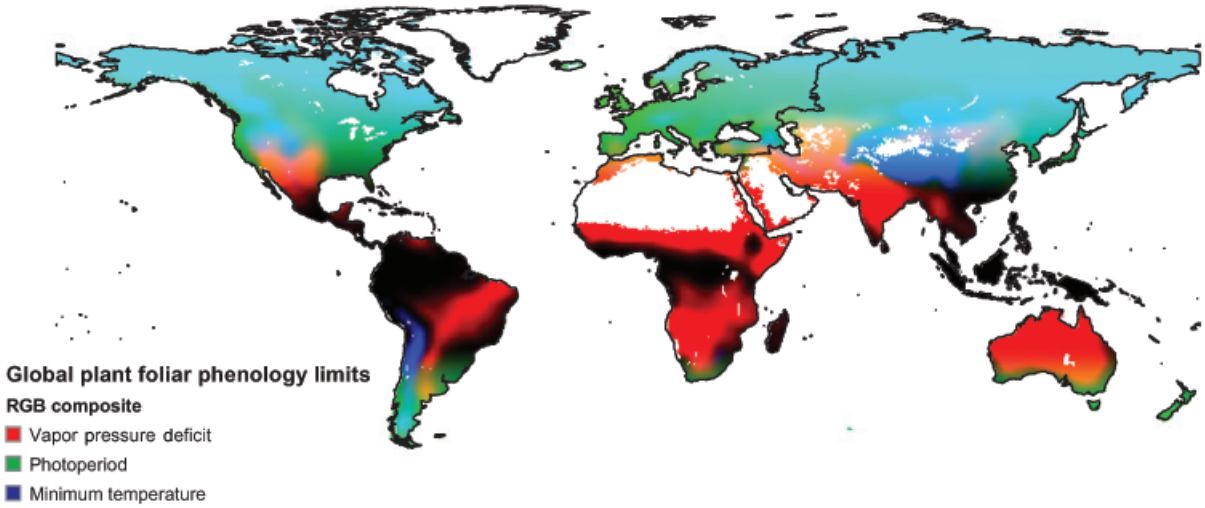

Fig. 5 Modeled regional constraints on phenology created from NCEP/NCAR weather data for the year 2000. In most regions, more than one variable limits phenology. The black area in the tropics indicates no seasonal constraints.

were observed. This may indicate inadequate model variables or parameters in these locations, but it could also suggest a difference in response time between locations. Shallow-rooted plants may respond more rapidly to environmental stimuli than deep-rooted plants. In this case, model predictions of earlier canopy initiation may not necessarily be wrong because we are comparing the results with radiometrically averaged NDVI values. If grasses account for only a small part of the signal, they may be hidden in the overall time series. We see a similar pattern at the Harvard Forest site where model predictions increase earlier than observed increases in NDVI. In similar locations, understory plants flush leaves up to 2 weeks earlier than overstory plants (Gill *et al.*, 1998; Augspurger & Bartlett, 2003), but the understory may contribute less than 20% to the total LAI (Rhoads *et al.*, 2002), suggesting that the NDVI response may be more dominated by larger vegetation.

Using VPD as a surrogate for precipitation has both advantages and disadvantages. The main advantage is that VPD is both continuous and easily calculated. Global phenology studies have cited the low reliability of precipitation and soil water potential data in the tropics as the reason for poor predictions of foliar phenology (Botta *et al.*, 2000), due in part to the discrete nature of precipitation. Precipitation, and its influence on soil water storage, is a major driver of tropical phenology. In many cases, leaf flush may be caused by a single precipitation event (Childes, 1989). If the data for that precipitation event were missing, this may introduce a serious bias into a model. VPD is a continuous variable and therefore would be less sensitive to a single missing value.

The primary disadvantage of using VPD as a surrogate for precipitation is that our model works on the assumption that changes in VPD are a direct result of seasonal precipitation changes. However, phenology itself may influence VPD through transpiration. Therefore, the main problem with using VPD in a prognostic phenology model is whether or not changes in VPD are a cause or effect: does VPD influence phenology or does phenology influence VPD? We know that there is a relationship between atmospheric water vapor pressure and the date of leaf emergence at landscape scales (Schwartz & Karl, 1990; Hayden, 1998) but the cause and effect of this relationship is not clear. If either advected moisture or precipitation raise vapor pressures independent of vegetation feedbacks, then changes in VPD could signal the onset of the rainy season. However, if VPD decreases are primarily a result of transpiration of newly flushed leaves, then this method would not work as a prognostic model. It would still work well as a monitoring model if using observations rather than predicted VPDs. If integrated into an ecosystem process model or a land-surface model, soil water potential could be substituted for the VPD control, using the same model framework. A similar method has been shown to adequately predict leaf area dynamics in some semiarid tropical regions (Jolly & Running, 2004) and should correct any model limitations caused by vegetation feedbacks.

Our model is independent of any particular application and therefore could be incorporated into larger modeling applications in a variety of ways. Although it goes against our argument of creating a continuous phenology model, we have shown that the model can still be used as a discrete trigger telling other simulation

models when to start growing leaves. Our model test at Harvard Forest showed good agreement between predicted and observed phenophase transition dates even when using the same parameters and logic used for all other sites. For this simple test, we defined a threshold GSI value above which we assumed that there is a plant canopy and below which you assume there is no plant canopy. Our choice of 0.5 appears to be a suitable threshold value. This cutoff value represents the proportion of days in the smoothing window (21 days in this case) in which conditions were suitable for a plant canopy. A value of 0.5 or greater simply means that at least half of the days in the smoothing window were sufficient to maintain a vegetative canopy. Predicted leaf onset dates at Harvard Forest were always greater than observations when we used 0.5 as the GSI cutoff. This bias might suggest that this simple cutoff may be too conservative. We encourage further exploration of this cutoff value, and we also suggest that this value may vary by species or biome. In theory, this threshold could also be used with monthly averages instead of daily running average values, allowing it to be incorporated into ecosystem process models that operate on monthly data such as the 3PG model (Landsberg & Waring, 1997).

This model could also be used to generate dynamic estimates of LAI by scaling the potential LAI for a site. The model by definition is bounded between 0 and 1, where 0 indicates times with a very low probability of a plant canopy and 1 indicates a very high probability of a canopy. Methods exist and have been tested in a variety of regions for determining the optimal LAI for a given site (Woodward, 1987; Nemani & Running, 1989). Our simple phenology model could be used to scale potential maximum LAI values for a site creating daily estimates of LAI throughout the growing season.

The model parameters used in this analysis are sufficient to reproduce large-scale differences in phenology throughout the world but we do not contend that these parameters are exactly the same everywhere. We understand that different species and biomes are sensitive to environmental conditions over different ranges of values (Larcher, 1995). Rather, we have attempted to provide a modeling framework and a simple set of parameters that sufficiently resolve the heterogeneity of phenology as observed from satellite data. Our efforts were geared towards creating a generalized phenology model, which is why we chose to develop a common set of parameters and not vary them by site. However, one should be able to tune the model to reproduce observed variation in phenology at local scales.

In addition to the fixed environmental parameters, we also chose a 21-day moving average because it produced the most general results. By averaging over 21 days, model results are less erratic. We tested a number of intervals from 7 to 21 days and found no appreciable difference among the smoothing intervals other than the desired effect of reducing erratic pulses of model predictions from extreme climatic events that were not indicative of average climatic conditions. It is plausible that different life forms respond differentially to changing environmental stimuli and that this parameter may be biome-specific, but the model seems to perform well for all biome types, suggesting our choice of a 21-day averaging window is sufficient in most locations. In fact, we improved correlations between GSI model predictions and NDVI at the two sites where the relationships were poorest were improved if we increased the moving window from 3 to 6 weeks. Correlations between GSI and NDVI at the Australia site improved from 0.57 to 0.75 and correlations at the Kalahari improved slightly from 0.74 to 0.8. These improvements were made without changing the parameters of the individual index calculations. Increasing the moving window length likely represents the longer term changes in soil water storage. The model assumes that changes in soil water availability are reflected as short-term changes in VPD; this moving window size may ensure that this assumption is met. However, throughout our discussion, we have emphasized the need for model generalization and that is why we chose present model simulations at each site using a 21-day moving window. Furthermore, the choice of smoothing window width also determines how fast the model transitions from one phenological condition to another, such as no leaves (0) to full canopies (1). Similar values have been reported in other studies that range from 21 to 31 days (Cleary & Waring, 1967; Van Wijk *et al.*, 2003).

Daily GSI values of one indicate that conditions were optimal for plant growth during that day. It is important to note that a GSI of one does not necessarily correspond to an NDVI value of one because GSI is independent of the vegetation cover and subsequent correlations between absolute GSI and NDVI values would be poor. However, if we sum daily GSI values over a calendar year, we can obtain a more mechanistic definition of growing season length and preliminary comparisons between these annual GSI sums and maximum annual NDVI indicate that they are strongly related. Therefore, it may be possible to scale daily GSI values to NDVI based on those annual totals.

Our map of phenological limiting factors is unique because it displays regions where limiting factors are either controlled by a single variable or an interaction of variables. Phenology is co-limited by multiple factors in many locations but these co-limitations have never been expressed spatially for the globe. This map is

consistent with other studies that suggests co-limits in a number of regions (Nilsen & Muller, 1981; White *et al*., 1997; Jame *et al*., 1998; Nemani *et al*., 2003). The black areas in the tropics define aseasonal climatic regions. In these areas, photoperiod is the only likely abiotic cue regulating canopy phenology. Indeed, in these areas, vegetation responds to photoperiod changes of as little as 15–30 min (Njoku, 1958; Borchert & Rivera, 2001). Pure temperature limits are rare and generally only seen in alpine regions such as the Andes of South America, the Rocky Mountains of North America, and the Tibetan plateau of central Asia. Pure water-limited phenology was more apparent over much of the globe. The high latitudes, where solar radiation and temperature are highly seasonal, show a mix of photoperiod and temperature limits which is consistent with previous research (Partanen *et al*., 1998). Midlatitude, temperate regions show more of a balance between photoperiod controls and low temperature limits. We hope that this map will better help researchers understand the limits to global phenological patterns.

We have presented a simple, meteorological data-based phenology model that can adequately predict the intra-annual dynamics of plant canopies at sites throughout the world using the same model logic and parameters with no *a priori* knowledge of the local vegetation or climate. We have demonstrated that this model is flexible enough to predict phenology regardless of the factors that control phenology regionally. We have used this model to generate a global map of climate limits to foliar phenology and we have found that it resolves spatial patterns of areas with vastly different phenological strategies. The model presented is simple and independent of any particular modeling framework and thus should be suitable for many global change applications.

Acknowledgements

We would like to thank Richard H. Waring, the editor and two anonymous reviewers for constructive comments on earlier versions of this manuscript. This research was supported in part by funds provided by the Joint Fire Science Program and the Rocky Mountain Research Station, Forest Service, US Department of Agriculture. We would like to thank John O'Keefe and the Harvard Forest for diligently maintaining the scientific quality phenology dataset used in this study. We also wish to thank the Distributed Active Archive Center (Code 902.2) at the Goddard Space Flight Center, Greenbelt, MD, 20771, for producing the data in their present form and distributing them. The original data products were produced under the NOAA/NASA Pathfinder program, by a processing team headed by Ms. Mary James of the Goddard Global Change Data Center; and the science algorithms were established by the AVHRR Land Science Working Group, chaired by Dr John Townshend of the University of Maryland. Goddard's contributions to these activities were sponsored by NASA's Mission to Planet Earth program.

References

Augspurger CK, Bartlett EA (2003) Differences in leaf phenology between juvenile and adult trees in a temperate deciduous forest. *Tree Physiology*, **23**, 517–525.

Bach CS (2002) Phenological patterns in monsoon rainforests in the Northern Territory, Australia. *Australian Journal of Ecology*, **27**, 477–489.

Borchert R, Rivera G (2001) Photoperiodic control of seasonal development and dormancy in tropical stem–succulent trees. *Tree Physiology*, **21**, 213–221.

Botta A, Viovy N, Ciais P *et al*. (2000) A global prognostic scheme of leaf onset using satellite data. *Global Change Biology*, **6**, 709–725.

Campbell GS, Norman JM (1998) *Environmental Biophysics*. Springer-Verlag, New York, NY.

Chase TN, Pielke RA, Kittel T *et al*. (1996) Sensitivity of a general circulation model to global changes in leaf area index. *Journal of Geophysical Research*, **101**, 7393–7408.

Childes SL (1989) Phenology of nine common woody species in semi-arid, deciduous Kalahari Sand vegetation. *Vegetatio*, **79**, 151–163.

Chuine I, Cour P (1999) Climatic determinants of budburst seasonality in four temperate-zone tree species. *New Phytologist*, **143**, 339–349.

Cleary BD, Waring RH (1967) Temperature: collection of data and its analysis for the interpretation of plant growth and distribution. *Canadian Journal of Botany*, **47**, 167–173.

de Bie S, Ketner P, Paasse M *et al*. (1998) Woody plant phenology in the West Africa savanna. *Journal of Biogeography*, **25**, 883–900.

Foley JA, Levis S, Prentice IC *et al*. (1998) Coupling dynamic models of climate and vegetation. *Global Change Biology*, **4**, 561–579.

Gill DS, Amthor JS, Bormann FH (1998) Leaf phenology, photosynthesis, and the persistence of saplings and shrubs in a mature northern hardwood forest. *Tree Physiology*, **18**, 281–289.

Granier C, Tardieu F (1999) Water deficit and spatial pattern of leaf development. Variability in responses can be simulated using a simple model of leaf development. *Plant Physiology*, **119**, 609–620.

Hakkinen R, Linkosalo T, Hari P (1998) Effects of dormancy and environmental factors on bud burst in *Betula pendula*. *Tree Physiology*, **18**, 707–712.

Hayden BP (1998) Ecosystem feedbacks on climate at the landscape scale. *Philosophical Transactions of the Royal Society of London*, **353**, 5–18.

Huffaker CB (1942) Vegetational correlations with vapor pressure deficit and relative humidity. *American Midland Naturalist*, **28**, 486–500.

IPCC (2001) *Climate Change 2001: The Scientific Basis. Contribution of the Working Group 1 to the Third Assessment Report of the IPCC*. Cambridge University Press, Cambridge.

Jame YW, Cutforth HW, Ritchie JT (1998) Interaction of temperature and daylength on leaf appearance rate in wheat and barley. *Agricultural and Forest Meteorology*, **92**, 241–249.

Jarvis P, Linder S (2000) Constraints to growth of boreal forests. *Nature*, **405**, 904–905.

Jolly WM, Running SW (2004) Effects of precipitation and soil water potential on drought deciduous phenology in the Kalahari. *Global Change Biology*, **10**, 303–308.

Justice CO, Townsend JRG, Holben BN *et al*. (1985) Analysis of the phenology of global vegetation using meteorological satellite data. *International Journal of Remote Sensing*, **4**, 369–385.

Kang S, Running SW, Lim J-H *et al*. (2003) A regional phenology model for detecting onset of greenness in temperate mixed forests, Korea: an application of MODIS leaf area index. *Remote Sensing of Environment*, **86**, 232–242.

Keeling CD, Chin JFS, Whorf TP (1996) Increased activity of northern vegetation inferred from atmospheric CO_2 measurements. *Nature*, **382**, 146–149.

Kistler R, Kalnay E, Collins W *et al*. (2001) The NCEP–NCAR 50-Year reanalysis: monthly means CD-ROM and documentation. *Bulletin of the American Meteorological Society*, **82**, 247–267.

Kramer K (1994) Selecting a model to predict the onset of growth of *Fagus sylvatica*. *Journal of Applied Ecology*, **31**, 172–181.

Landsberg JJ, Waring RH (1997) A generalized model of forest productivity using simplified concepts of radiation-use efficiency, carbon balance and partitioning. *Forest Ecology and Management*, **95**, 209–228.

Larcher W (1995) *Physiological Plant Ecology*. Springer-Verlag, Heidelberg.

Larcher W, Bauer H (1981) Ecological significance of resistance to low temperature. In: *Encyclopedia of Plant Physiology*, **Vol. 12A** (eds Lange OL, Nobel PS, Osmond CB, Ziegler H), pp. 403–437. Springer-Verlag, Berlin.

Lechowicz MJ (2001) Phenology. In: *Encyclopedia of Global Environmental Change* (ed. Canadell J, Mooney HA), **Vol. 2**. Wiley, London.

Levitt J (1980) *Responses of Plants to Environmental Stresses*. Academic Press, New York.

Lieberman D (1982) Seasonality and phenology in a dry tropical forest in Ghana. *Journal of Ecology*, **70**, 791–806.

Lieth H (1974) *Phenology and Seasonality Modeling*. Springer, Berlin, Germany.

Lovell JL, Graetz RD (2001) Filtering Pathfinder AVHRR Land NDVI data for Australia. *International Journal of Remote Sensing*, **22**, 2649–2654.

Matsumoto K, Ohta T, Irasawa M *et al*. (2003) Climate change and extension of the *Ginkgo biloba* L. growing season in Japan. *Global Change Biology*, **9**, 1634–1642.

Menzel A (2002) Phenology: its importance to the global change community. *Climatic Change*, **54**, 379–385.

Menzel A, Fabian P (1999) Growing season extended in Europe. *Nature*, **397**, 659.

Monteith JL, Unsworth MH (1990) *Principles of Environmental Physics*. Edward Arnold, New York, NY.

Mott KA, Parkhurst DF (1991) Stomatal responses to humidity in air and helox. *Plant Cell and Environment*, **14**, 509–515.

Myneni RB, Keeling CD, Tucker CJ *et al*. (1997) Increased plant growth in the northern latitudes from 1981 to 1991. *Nature*, **386**, 698–702.

Myneni RB, Maggion S, Iaquinta J *et al*. (1995) Optical remote sensing of vegetation: modelling, caveats and algorithms. *Remote Sensing of Environment*, **51**, 169–188.

Nemani RR, Keeling CD, Hashimoto H *et al*. (2003) Climate-driven increases in global terrestrial net primary production from 1982 to 1999. *Science*, **300**, 1560–1563.

Nemani RR, Running SR (1989) Testing a theoretical climate–soil–leaf area hydrologic equilibrium of forests using satellite data and ecosystem simulation. *Agricultural and Forest Meteorology*, **44**, 245–260.

Nilsen ET, Muller WH (1981) Phenology of the drought–deciduous shrub *Lotus scoparius*: climatic controls and adaptive significance. *Ecological Monographs*, **51**, 323–341.

Njoku E (1958) The photoperiodic response of some Nigerian plants. *Journal of the West African Science Association*, **4**, 99–111.

Olson DM, Dinerstein E, Wikramanayake ED *et al*. (2001) Terrestrial ecoregions of the World: a new map of life on Earth. *BioScience*, **51**, 933–938.

Osonubi O, Davies WJ (1980) The influence of plant water stress on stomatal control of gas exchange at different levels of atmospheric humidity. *Oecologia*, **46**, 1–6.

Partanen J, Koski V, Hänninen H (1998) Effects of photoperiod and temperature on the timing of bud burst in Norway spruce (*Picea abies*). *Tree Physiology*, **18**, 811–816.

Peñuelas J, Filella I, Zhang X *et al*. (2004) Complex spatiotemporal phenological shifts as a response to rainfall changes. *New Phytologist*, **161**, 837–846.

Rhoads AG, Hamburg SP, Fahey TJ *et al*. (2002) Effects of an intense ice storm on the structure of a northern hardwood forest. *Canadian Journal of Forest Research*, **32**, 1763–1775.

Rosenthal SI, Camm EL (1997) Photosynthetic decline and pigment loss during autumn foliar senescence in western larch (*Larix occidentalis*). *Tree Physiology*, **17**, 767–775.

Salah H, Tardieu F (1996) Quantitative analysis of the combined effects of temperature, evaporative demand and light on leaf elongation rate in well-watered field and laboratory-grown maize plants. *Journal of Experimental Botany*, **47**, 1689–1698.

Schwartz MD (1999) Advancing to full bloom: planning phenological research for the 21st century. *International Journal of Biometeorology*, **42**, 113–118.

Schwartz MD, Karl TR (1990) Spring phenology: nature's experiment to detect the effect of 'green-up' on surface maximum temperatures. *Monthly Weather Review*, **118**, 883–890.

Schwartz MD, Reiter BE (2000) Changes in North American spring. *International Journal of Climatology*, **20**, 929–932.

Sellers P, Los SO, Tucker CJ *et al*. (1996) A revised land surface parameterization (SiB2) for atmospheric GCMs, II, The generation of global fields of terrestrial biophysical parameters from satellite data. *Journal of Climate*, **9**, 706–737.

Sparks TH, Carey PD (1995) The responses of species to climate over two centuries, 1736–1947: an analysis of the Marsham phenological record. *Journal of Ecology*, **83**, 321–329.

Tenhunen JD, Hanano R, Abril M *et al*. (1982) The control by atmospheric factors and water stress of midday stomatal closure in *Arbutus unedo* growing in a natural macchia. *Oecologia*, **55**, 165–169.

Thornton PE, Running SW, White MA (1997) Generating surfaces of daily meteorological variables over large regions of complex terrain. *Journal of Hydrology*, **190**, 241–251.

Van Wijk MT, Williams M, JA, GR (2003) Interannual variability of plant phenology in tussock tundra: modelling

interactions of plant productivity, plant phenology, snowmelt and soil thaw. *Global Change Biology*, **9**, ;743–758.

Waring RH (1969) Forest plants of the eastern Siskiyous: their environmental and vegetational distribution. *Northwest Science*, **43**, 1–17.

White MA, Thornton PE, Running SW (1997) A continental phenology model for monitoring vegetation response to interannual climatic variability. *Global Biogeochemical Cycles*, **11**, 217–234.

White MA, Thornton PE, Running SW *et al*. (2000) Parameterization and sensitivity analysis of the BIOME–BGC terrestrial ecosystem model: net primary production controls. *Earth Interactions*, **4**, 1–85.

Woodward FI (1987) *Climate and Plant Distribution*. Cambridge University Press, Cambridge.

Zimmerman MH (1964) Effect of low temperature on ascent of sap in trees. *Plant Physiology*, **39**, 568–572.